Biomimetic Fish-like Underwater Robot for Shallow Water Applications.

Madis Listak
Dept. of Computer Engineering
Tallinn University of Technology
Raja 15, 12618 Tallinn
Estonia
Madis.Listak@netbell.ee

David Pugal, Maarja Kruusmaa
Insitute of Technology
Tartu University
Nooruse 1, 50411, Tartu
Estonia
{David.Pugal, Maarja.Kruusmaa}@ut.ee

Abstract - **This paper describes the prototype of a fishlike biomimetic underwater robot. The design considerations of the vehicle are task-specific. The vehicle is designed for visual inspection in shallow waters with low visibility and volatile sediments. In those conditions a vehicle with thrusters would cause too much turbulence. We propose a biologically inspired underwater vehicle that uses fins for propulsion and operates in towed, tethered remotely operated and autonomous modes.**
In this paper we describe the design of the vehicle and experiments in a towed mode. In the towed mode the vehicle is dragged after a boat at low speed while staying close to the bottom for visual inspection. We show that it can follow the ground profile at a speed suitable for visual inspection.

Index Terms – underwater robotics, biologically inspired robot fish, environmental monitoring.

I. Introduction

Fishes and other aquatic animals inspire many underwater robots. The reasons for that are their swimming efficiency, great maneuverability, trajectory following and station keeping capability.

Biomimetic underwater devices reported so far include a robotic tuna fish [1, 2], control of a fish by means of a caudal fin [4] or pectoral fins [5]. Most of biomimetic underwater vehicles mimic carangiform swimming (propulsion through the water with oscillating movements of the tail and the rear part of the body) [7][boxfish][flexible bodies]. Other types of swimming are also implemented, for example anguilliform (eel-like) locomotion [8][9,10] and locomotion with the help of elongated pectoral fins [11, 12].

The aim of this study is to design an underwater robot with a fish-like locomotion for practical environmental monitoring purposes. As such, the goal is not to mimic aquatic animals or to implement dynamics and kinematics of swimming as closely as possible but rather to make use of these features in practical applications.

As an application area we consider visual inspection of shallow water bodies with low visibility. Many inland water bodies fall into this category (lakes, rivers, ponds, bogs) as well as shallow and closed seas. For example The Baltic Sea is considered to be an exploitation area of such a device. It is very shallow and turbid. At the same time it is one of the most severely polluted seas in the world and according to EU directives is under regular environmental monitoring. At present visual transect surveys are done by divers.

The bottom of this kind of water bodies is usually covered with thick layer of mud or extremely volatile detritus (small particles of zoo- and phytoplankton). This poses a difficult problem. On the one hand the visibility is very low and one has to stay close to the bottom for visual inspection. On the other hand, locomotion in vicinity of the muddy bottom would decrease visibility. We therefore need a device, which creates as little turbulence as possible when moving.

Thrusters are efficient for fast locomotion, they are also commercially available and therefore inexpensive, but their operation creates a strong water stream. For the above-described application, in contrast, there is no need for fast locomotion but rather for good maneuverability and station keeping capability for close visual inspection. Locomotion of fins creates considerably less turbulence. Also it is possible to achieve good maneuverability by adding control surfaces.

The devices for visual inspection reported so far are too big and heavy for very shallow waters [13] and they almost exclusively used thrusters for locomotion [14]. We propose an alternative concept of an underwater robot. The design considerations of this device are based on task requirements. The vehicle should be able to operate in a very shallow water (1 m – 20 m) with a low visibility, create little turbulence, should be operated easily by only one person, be lightweight and inexpensive.

The goal is to build a vehicle that can be operated in 3 modes, towed mode, remotely operated mode and fully autonomous mode. At present we test the vehicle in the towed mode and this paper represents the first experimental results.

The rest of the paper is organized as follows. Section II presents the overview of the vehicle. In Section III we analyze the vehicle in a towing mode to find its capability to surface and submerge. Section IV represents the results of the field tests. The results show that the vehicle is able to follow the bottom profile when towed at low speed and is stable in still water.

II. VEHICLE OVERVIEW

This paper describes our second prototype vehicle (Fig. 1) that is designed considering the test results of the first prototype [ref to authors removed].

Fig 1. Second prototype without protective cover and with towing rod attached.

The main characteristics of the prototype are the following:

Weigh of the robot	16 kg
Length of the body	1,5 m
Width of the body	0,6 m
Electrical power	24 V

Our long-term goal is to design a vehicle capable of operating in three different modes with a varying degree of autonomy. In a towed mode the vehicle is dragged behind a boat at low speed and it should be able to follow the bottom profile at height sufficient for visual inspection. The tethered remotely controlled mode is to be used for a close visual inspection. The vehicle in an autonomous mode should be also capable of navigation and operates on an on-board power supply.

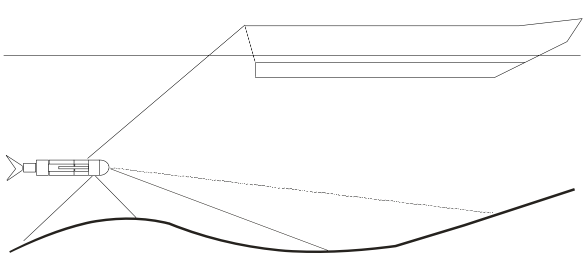

Fig 2. Operation in towing mode.

At present the vehicle is tested in a towed mode as shown in Fig 2. but is also capable of autonomous operation by propulsion of the caudal fin.

The towed mode is tested first for several reasons. First of all, in this mode the vehicle is presumably easiest to control. Second, our consultations with environmental scientists suggest that it satisfies the requirements of the target user group. The towed mode is best suited for visual transect surveys to replace the human diver. It permits covering long distances at speed suitable for visual inspection. As the problems of energy autonomy and underwater navigation do not have to be addressed in this mode we hope to demonstrate soon the usability of an operational prototype. Also, consultations with the potential users show even that a tethered mode is preferred to autonomous since environmental researchers suffer significant losses of their equipment because of bad weather conditions.

III. MECHANICAL STRUCTURE

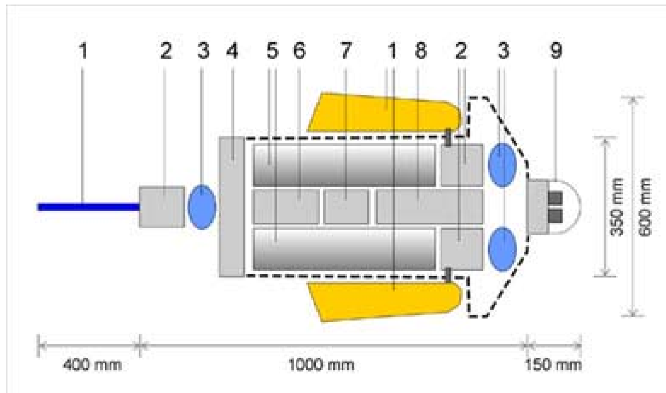

Fig. 3. Internal layout (1 – fins; 2 - motors; 3 - buoyancy control; 4 - air supply; 5 - batteries; 6 - gyro and inertial sensor; 7 – OMAP ; 8 – control electronics; 9 - camera and sonar head;)

The body of robot is made of an extruded polyester sheet attached to the aluminum and stainless steel frame. The overall schematic is described in figure 3. The robot has a compressed air supply of 200 bar for 76 l of air. This air is used for buoyancy control. The robot has three buoyancy control chambers – two of them are in the front and one in the back section. The airflow is regulated with 7 valves. Each buoyancy control chamber has an inlet valve and an outlet valve. One valve is equalizing pressure between two front chambers. The front chambers are used to change the orientation of the body from vertical to horizontal and back. Equalizing the pressure between these chambers helps to stabilize the body.

The robot is equipped with sonar and a color camera. These instruments are located in the front part and can be used in any orientation. For towing missions we have retractable towing rod what is connected to the front part so that it permits the vehicle to roll. The rod is in turn connected to a towing cable. Two battery packs supply 24 V for 3 dc motors driving fins through the reductors. The robot has one tail fin for steering and main propulsion and two side fins for additional propulsion and maintaining the depth. The fins are made of soft plastic to withstand impacts. The center of mass of the vehicle can be adjusted by changing the position of the batteries inside their shells. Electronics is located between the batteries to have better protection from environment and impacts. A gyro is located in the center of mass to reduce errors.

IV. ELECTRONICS AND CONTROL

The control system has 12 V backup power. The conceptual control system architecture is described in Fig. 4. The robot's mission control is performed by Texas Instruments 16-bit MSP430 microcontroller. This controller is responsible for controlling actuators and measuring devices. Its conceptual control loop is described in Fig. 5. The robot has also a StrongARM based OMAP which is used for recording the video stream from the color camera. It also reads data from Imagenex 852 echo sounder and is responsible for reprogramming the MSP 430 controller. Communication with the boat is also maintained through OMAP using an ethernet cable and TCP/IP protocol. For navigation we use 6 DOF inertial measurement device and 3 axes magnetometer from Rotomotion.

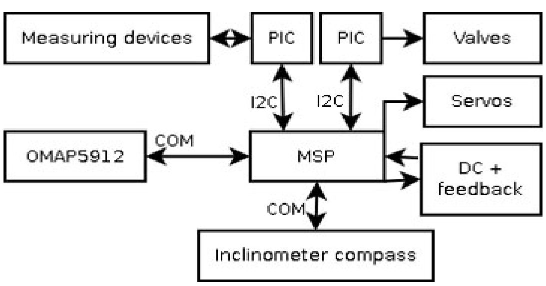

Fig. 4. Conceptual control system

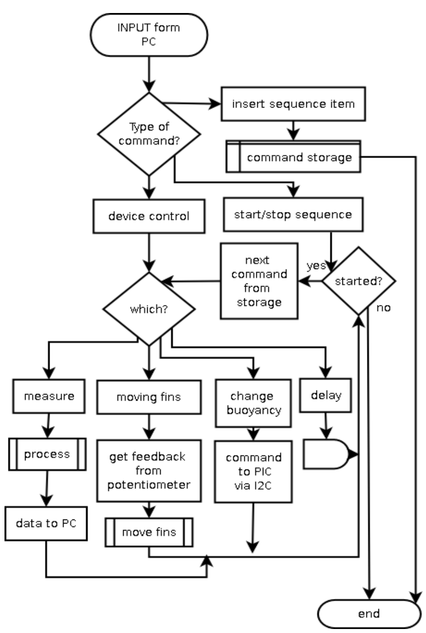

Fig. 5. Communication flow in MSP430 microcontroller

V. MODELING AND EXPERIMENTAL SETUP

For predicting robots performance and behavior we developed a theoretical model that describes submerging and surfacing. For that purpose we measured the drag coefficient of the body.

Experiments were made in a pond shown in Fig. 6. A 10m long track was marked to measure distance. In the first test we measured the speed of the robot and calculated the drag force according to Eq. 6.

Fig. 6. Measuring the drag force

A. Measuring and modeling the drag force.

We found drag force experimentally by dragging the robot with constant force and registering average speed of the robot. The drag coefficient

$$_R = \frac{2 \cdot F_{dR}}{\rho \cdot v^2 \cdot S_R} \qquad (1)$$

where S_R stands for cross section area of the robot and is approximately 0.088 m^2

TABLE I
DRAG FORCES, COEFFICIENTS AND MEASURED SPEEDS

Applied drag force (N)	*Speed (m/s)*	*Drag coefficient*
10	0.46	1.09
15	0.6	0.97
20	0.69	0.98

The results of the drag force measurements are represented in Table I and show that the average drag coefficient is 1.

Lift force generated by fins causes vertical movement of the robot. In Fig 7, *F* is the constant force applied to the robot through the towing rod, F_L is the lift force, F_{dF} is the drag force caused by fins and F_{dR} is the drag force caused by the body. As γ didn't change considerably during the experiments it is considered to have a constant value $\gamma = 30^o$.

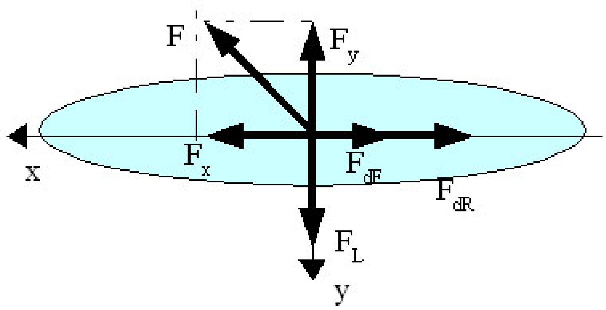

Fig. 7. Forces applied to the robot

According to [15] for a small angle of attack of a flat surface moving in continuous environment, the lift coefficient is approximately:

$$ {}_L = \frac{4 \cdot C_{Lmax} \cdot \alpha}{\pi} \quad (2) $$

and the drag coefficient is

$$ {}_D = \frac{4 \cdot C_{Dmax} \cdot \alpha \cdot \tan(\alpha)}{\pi} \quad (3) $$

where C_{Dmax} =1,2 and C_{Lmax} =1,38 for a flat surface. The angle of attack of a fin in our experiments is 30 deg. We can calculate lift and drag forces for a pair of fins of the robot.

$$ F_L = \frac{4}{\pi} \cdot C_{Lmax} \cdot \alpha \cdot \rho \cdot S_{fin} \cdot v_x^2 \quad (4) $$

and

$$ F_{dF} = \frac{4}{\pi} \cdot C_{Dmax} \cdot \alpha \cdot \tan(\alpha) \cdot \rho \cdot S_{fin} \cdot v_x^2 \ . \quad (5) $$

The drag force of the robot is

$$ F_{dR} = \frac{1}{2} \cdot C_R \cdot \rho \cdot S_R \cdot v_x^2 \quad (6) $$

where C_R is the drag coefficient of a horizontally moving robot and S_R is the cross section area of the robot. Simply we get v_x as function on F_x

$$ v_x(F_x) = \sqrt{\frac{F_x}{\frac{4 \cdot \rho}{\pi} \cdot C_{Dmax} \cdot \alpha \cdot \tan(\alpha) \cdot S_{fin} + \frac{1}{2} \cdot \rho \cdot C_R \cdot S_R}} \quad (7) $$

Thus the theoretical calculations show that the velocities corresponding to the applied forces {10 N, 15 N, 20 N} are {0.35 m/s, 0.43 m/s, 0.49 m/s}.

Test results of the drag force and speed measurements are represented in Table I. The results show that the theoretical calculations are very close to the experimental data.

B. Measuring and modeling the submerging speed.

If we consider the surface area of the robot flat we get drag force equation for vertical movement:

$$ F_{dV} = \frac{4}{\pi} \cdot C_{Lmax} \cdot \alpha \cdot \rho \cdot S_{fin} \cdot v_x^2 - F \cdot \sin(\gamma) = \frac{1}{2} \cdot C_{Dmax} \cdot \rho \cdot S_{R2} \cdot v_y^2 \quad (8) $$

where S_{R2} is the surface area of the robot. If the difference between the lift force F_L and the vertical applied force F_y is balanced by F_{dV}, the vertical speed of the robot will be v_y . Theoretical values corresponding to applied forces {10 N, 15 N, 20 N} are {0.4 m/s, 0.49 m/s, 0.57 m/s}.

According to these theoretical calculations the submerging and surfacing capability satisfies the requirements of the application. For example, if the robot is towed behind a boat with the speed 1.8 km/h, which is a speed suitable for visual transect surveys, and it's drag force is about 20 N, then along the vertical distance 1 m the robot is able to submerge vertically 1.1 m and to surface 1.3 m, e.g. more than by 45 degrees angle.

The next series of experiments were conducted to measure the robot's submerging capability. In these experiments the buoyancy was set to neutral and side fins were set to submerging position under 30 degrees angle of attack. The robot was towed with a constant force and time and depth were recorded. The experimental results are represented in Table II.

TABLE II
SUBMERGING SPEEDS

Applied drag force (N)	*Speed (m/s)*
10	0.16
15	0.2
20	0.2

The submerging capability of the robot appeared not to be as good as it could be expected from the theoretical results. For the same example represented in Section VI (speed 1.8 km/h, drag force is about 20 N, horizontal distance 1 m) the robot submerges vertically 0.4 m while the theoretical calculations suggest the depth of 1.1 m.

Differences between theoretical values presented in the previous section and experimental values are probably due to the fact that body can act also as a fin. While dragging the body, even slight orientation change of the body can cause extra lift force. For instance flat body with the angle of attack equal 5 degrees and with surface area 0.35 m^2 moving with velocity 0.5 m/s can cause extra lift force approximately 10 N.

Thus the actual angle of submerging and surfacing is less that theoretically expected but is nevertheless sufficient for most of applications and can be improved by adjusting the center of mass of the robot so that the angle of the body will change and the additional lift force is decreased.

The tests also proved that the robot in a towed mode is sufficiently stable in still water. It maintained a constant yaw and pitch angle even without feedback correction.

VI. CONCLUSIONS AND FUTURE WORK

This paper described a prototype of a fish-like underwater robot for shallow water applications. The biomimetic design of the vehicle makes it suitable for visual inspection of a bottom with volatile sediments and low visibility.

For fast visual inspection the vehicle is towed behind a boat while keeping a constant height from the bottom. This paper analyzed the robot's ability to follow the ground profile. The calculations show that the robot is able to submerge and surface fast enough even if the bottom is rather uneven. The calculations were confirmed by experimental data. The submerging speed gained form the experimental data was somewhat less than estimated by theoretical calculations but can be presumably increased by adjusting the center of mass and the yaw angle.

The experiments also reviled that in the towed mode the vehicle is sufficiently stable in still water. Our next step is to implement the feedback control of the robot by using forward and down looking sonar signals, inclinometers and gyro for feedback. The goal is to make the vehicle stable also in currents and waves and to follow the ground profile.

REFERENCES

[1] E. Kim, Y. Youm, "Design and Dynamic Analysis of Fish Robot PoTuna." *Proceedings of the 2004 IEEE Int. Conf. on Robotics and Automation (ICRA 2004),* New Orleans, LA, April 2004, pp. 4887-4892.

[2] J.M.Anderson, M.S. Triantafyllou, P.A.Kerrebrock. "Concept Design of a Flexible-Hull Unmanned Undersea Vehicle." *Proceedings of the Int. Offshore and Polar Engineering Conf.*,1997, pp. 82-88.

[3] D. McFarland, I. Gilhespy, E. Honary, "DIVEBOT: A Diving Robot with a Whale-like Buoyancy Mechanism." Robotica, Vol. 21, 2003, pp. 385 – 398.

[4] M. Mojarrad, "AUV Biomimetic Propulsion," in *Proceedings of OCEANS 2000 MTS/IEEE Conference and Exhibition*, vol. 3 , 11-14 Sept. 2000, pp. 2141 – 2146

[5] N. Kato, T. Inaba, "Guidance and Control of Fish Robot with Apparatus of Pectoral Fin Motion." *Proceedings. of the 2001 IEEE Int. Conf. on Robotics and Automation*, Leuven, Belgium, May 1998, pp. 446 – 451.

[6] Y. Terada, I. Yamamoto. "An Animatronics System Including Lifelike Robotic Fish." Proc. Of the IEEE, Vol. 92. No. 11, November 2004, pp. 1814-1820.

[7] J. Yu, M. Tan, S.Wang, E.Chen. „Development of a Biomimetic Robotic Fish and Its Control." IEEE Trans. On Systems, Man and Cybernetics, Vol. 34, No. 4, August 2004, pp. 1798-1810.

[8] K. A. McIsaac, J.P.Ostrowski, "Motion Planning for Anguilliform Locomotion." IEEE Trans. On Robotics and Automation, Vol. 19, No.4, August 2003,.pp. 637 – 652.

[9] Chablat, Damien; Wenger, Philippe "Design of a Spherical Wrist with Parallel Architecture- Application to Vertebrae of an Eel Robot" *Conf. on Robotics and Automation (ICRA 2005),), Barcelona, Spain, April 18-22 2005.*

[10] Crespi, Alessandro; Badertscher, A. Guignard, A. Ijspeert, Auke Jan "Swimming and Crawling with an Amphibious Snake Robot" *Conf. on Robotics and Automation (ICRA 2005),), Barcelona, Spain, April 18-22 2005.*

[11] M. Sfakiotakis, D.M. Lane, J.B.c. Davies, J.B.c. "An Experimental undulating-fin device using the parallel Bellows Actuator." *Proc. of the 2001 IEEE Int. Conf. on Robotics and Automation,* Seoul, Korea, May 21-25, 2001, pp. 2356-2362.

[12] Andres Punning, Mart Anton, Maarja Kruusmaa, Alvo Aabloo, "A Biologically Inspired Ray-like Underwater Robot with Electroactive Polymer Pectoral Fins", *Proc. of the Int. IEEE Conf. Mechatronics and Robotics 2004 (MechRob'04),* Vol. 2, pp. 241 - 245, 13. - 15. Sept. 2004, Aachen.

[13] Jin-Kyu Choi, Hiroshi Sakai and Toshinari Tanaka "Autonomous Towed Vehicle for Underwater Inspection in a Port Area" " *Conf. on Robotics and Automation (ICRA 2005),), Barcelona, Spain, April 18-22 2005.*

[14] Dunbabin, Matthew; Roberts, Jonathan; Usher, Kane; Winstanley, Graeme; Corke, Peter "A Hybrid AUV Design for Shallow Water Reef Navigation" *Proceedings of the 2004 IEEE Int. Conf. on Robotics and Automation (ICRA 2005), Barcelona, Spain, April 18-22 2005.*

[15] Horner, Dr. Sighard F., "Fluid-Dynamic Drag: Practical Information on Aerodynamic Drag and Hydrodynamic Resistance, 1965."